# Heat transfer analysis of electrically conductive Blasius flow of Casson nanofluid in a porous medium

Ravinder Kumar
Department of Mathematics, Chandigarh University, SAS Nagar (Mohali), Punjab, India

**Abstract:** In this article, we have discussed the behavior of electrically conducted Blasius flow of non-Newtonian nanofluid under the influence of Forchheimer equation. For non-Newtonian nature of the nanofluid, the Casson model is employed. Heat and mass transfer rates are analyzed under the influence of heat source and sink devices. The Governing boundary layer PDEs are converted to ODEs under proper similarity transformations. RK45 numerical scheme along with the Newton-Raphson shooting technique is utilized to solve the set of ODEs. The effects of dimensionless parameters on velocity, temperature, concentration, heat transfer rate, and mass transfer rate are presented via figures.

**Keywords**: Forchheimer equation, Casson nanofluid, Magnetic field, Heat source/sink, Shooting method

## 1. Introduction

Free stream analysis of a 3D Casson nanofluid flowing through forchheimer extended Darcy model for the porous medium is made in this investigation. The magnetic field is considered to be influencing along with the heat source/sink.

The concept of Constantly moving fluid over a motionless surface is observed in many real-life fluids flows [1]. It is important to control the thickness and separation of the boundary layer which is mainly dominated by friction [2]. Ridha [3] computed the solution of a 3Dl Blasius transport numerically. Kachanov and Michalke [4] compared the experimental results with theoretical solutions for the instability of a 3-D Blasius transport. Tsigklifis and Lucey [5] conferred an approach for the inspection of the comprehensive stability of 3D disorders in Blasius transport.

We interact with non-Newtonian fluids in our day-to-day life like honey, blood, toothpaste, paints, juices, and shampoos. These kinds of fluids are flexible and observe the transformation from fluid to solid depending upon relaxation and observation time [12]. Researchers have found new models over time to predict the properties of a non-Newtonian fluid out of which the Casson model is influencing and have unique properties(shear thinning/thickening).

The applications of electrically conducting fluids are found in geophysics, engineering, astrophysics, MHD accelerator, and many more. The magnetic field can restrain the velocity, concentration, and temperature of a fluid. Many researchers have examined this concept in a different types of physical problems. Magnetic field influences on a non-radiative 3Dl flow due to a pressure-supported torus is inspected by Hawley et al. [8]. The magnetic-force-free concept is introduced by Chandrasekhar and Kendall [6]. MHD model for three-dimensional flow in Titans plasma environment is inspected by [7]. Hayat et al. [9] investigated an unsteady MHD three-dimensional flow over a stretching surface. Rakesh et al. [11] analyzed MHD flow in the stagnation region and in presence of velocity/thermal slip.

Fluid Transport through pores and their connectedness is an undetachable part of fluid dynamics [13]. Flow through these geometries has vast applications in plastic-films, the extrusion of polymer, human bones, extraction of petroleum, turbine blades and many more [14]-[15]. Some other important research works in this field are [17]-[19].

## 2. Mathematical formulation

In this study, we have considered a 3D flow of Casson nanofluid under Blasius conditions, in the presence of Darcy-Forchheimer model of porous surface. Inertia coefficient of porous medium in $x$ and $y$ directions are taken as $F_1 = \frac{c_b}{x\sqrt{K_1}}$ and $F_2 = \frac{c_b}{y\sqrt{K_1}}$ respectively. The system of nanofluid governing equations along with boundaries restrictions formulated as [12]:

$$v_{1_x} + v_{2_y} + v_{3_z} = 0, \tag{1}$$

$$v_1 v_{1_x} + v_2 v_{1_y} + v_3 v_{1_z} = \nu_f \left(1 + \frac{1}{\beta}\right) v_{1_{zz}} + V_1 V_{1_x} + V_2 V_{1_y} - \frac{\nu_f}{K_1}(v_1 - V_1) - F_1(v_1^2 - V_1^2) - \frac{\sigma_f B^2}{\rho_f}(v_1 - V_1), \tag{2}$$

$$v_1 v_{2_x} + v_2 v_{2_y} + v_3 v_{2_z} = \nu_f \left(1 + \frac{1}{\beta}\right) v_{2_{zz}} + V_1 V_{2_x} + V_2 V_{2_y} - \frac{\nu_f}{K_1}(v_2 - V_2) - F_1(v_2^2 - V_2^2) - \frac{\sigma_f B^2}{\rho_f}(v_2 - V_2), \tag{3}$$

$$v_1 \alpha_x + v_2 \alpha_y + v_3 \alpha_z = T_a \alpha_{zz} + \kappa(B_d \alpha_z \beta_z + A_d \alpha_z^2) + q''' \tag{4}$$

$$v_1 \beta_x + v_2 \beta_y + v_3 \beta_z = B_d \beta_{zz} + A_d \alpha_{zz} \tag{5}$$

$$\left.\begin{array}{l} v_1 = v_{1_w}, \quad v_2 = v_{2_w}, \quad v_3 = 0, \quad \alpha = \alpha_w, \quad \beta = \beta_w \quad at \quad z = 0 \\ v_1 = V_1, \quad v_2 = V_2, \quad \alpha \to \alpha_\infty, \quad \beta \to \beta_\infty \quad at \quad z \to \infty \end{array}\right\}. \tag{6}$$

In the above equations, $q''' = \frac{Q}{\rho c_p}(\alpha - \alpha_\infty)$

PDEs are transformed to ODEs utilizing the following similarity transformations.

$$v_1 = ax\varphi_{1'}, \quad v_2 = ay\varphi_{2'}, \quad v_3 = -\sqrt{av}(\varphi_1 + \varphi_2), \quad \varphi_3 = \frac{\alpha - \alpha_\infty}{\alpha_w - \alpha_\infty}, \quad \varphi_4 = \frac{\beta - \beta_\infty}{\beta_w - \beta_\infty} \quad \text{where} \quad \eta = \sqrt{\frac{a}{\nu}}z$$

The obtained coupled ordinary differential equations are

$$\left(1 + \frac{1}{\beta}\right)\varphi_{1_{\eta\eta\eta}} + (\varphi_1 + \varphi_2)\varphi_{1_{\eta\eta}} - \left(\frac{1}{Da} + M\right)(\varphi_{1_\eta} - \lambda_3) - Fr(\varphi_{1_\eta}^2 - \lambda_3^2) + \lambda_3^2 - \varphi_{1_\eta}^2 = 0 \tag{7}$$

$$\left(1 + \frac{1}{\beta}\right)\varphi_{2_{\eta\eta\eta}} + (\varphi_1 + \varphi_2)\varphi_{2_{\eta\eta}} - \left(\frac{1}{Da} + M\right)(\varphi_{2_\eta} - \lambda_4) - Fr(\varphi_{2_\eta}^2 - \lambda_4^2) + \lambda_4^2 - \varphi_{2_\eta}^2 = 0 \tag{8}$$

$$\varphi_{3''} + Pr[Nb\varphi_{4'} + Nt\varphi_{3'}]\varphi_{3'} + Pr(\varphi_1 + \varphi_2)\varphi_{3'} + Q^*\varphi_3 = 0 \tag{9}$$

$$\varphi_{4''} + Sc(\varphi_1 + \varphi_2)\varphi_{4'} + Nr\varphi_{3''} = 0 \quad (10)$$

The deduced restrictions are

$$(\varphi_1 + \varphi_2)(\eta) = 0, \quad \varphi_{1'}(\eta) = \lambda_1, \quad \varphi_{2'}(\eta) = \lambda_2, \quad \varphi_3(\eta) = 1, \quad \varphi_4(\eta) = 1, \quad \text{as} \quad \eta \to 0$$
$$\varphi_{1'}(\eta) = \lambda_3, \quad \varphi_{2'}(\eta) = \lambda_4, \quad \varphi_3(\eta) = 0, \quad \varphi_4(\eta) = 0, \quad \text{as} \quad \eta \to \infty \quad (11)$$

Notations and dimensionless parameters

$$\kappa = \frac{(\rho c_p)_s}{(\rho c_p)_f}, \quad A_d = \frac{T_d}{\alpha_\infty}, \quad Da = \frac{aK_1}{\nu_f}, \quad Q^* = \frac{Q}{a\rho c_p}, \quad Nt = \frac{\kappa A_d(\alpha_w - \alpha_\infty)}{\nu_f}, M = \frac{\sigma_f B^2}{\rho_f a}$$

$$Sc = \frac{\nu_f}{B_d}, \quad Fr = \frac{c_b}{\sqrt{K}}, \quad Nr = \frac{Nt}{Nb}, \quad Pr = \frac{\nu_f}{\alpha_f}, \quad Nb = \frac{\kappa B_d(\beta_w - \beta_\infty)}{\nu_f},$$

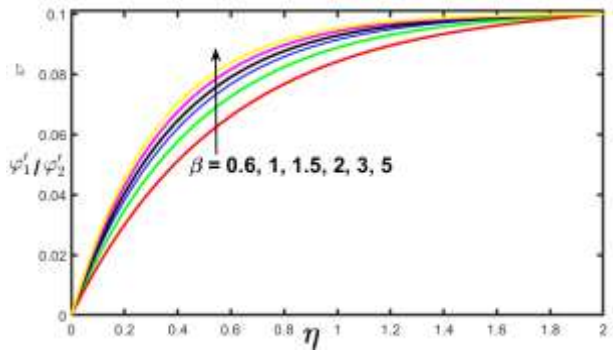


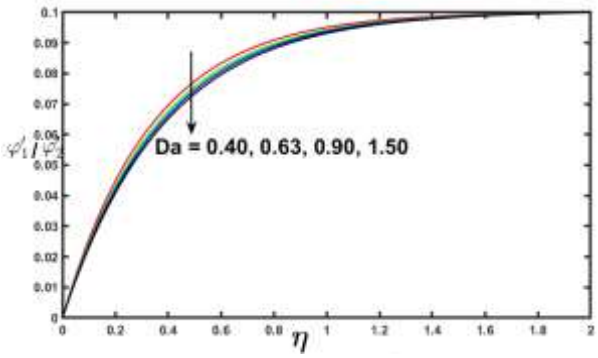


Fig.1: Variability of $\varphi_{1'}$ and $\varphi_{2'}$ with $\beta$. Fig.2: Variability of $\varphi_{1'}$ and $\varphi_{2'}$ with $Da$.

## 3. Numerical Method

Newton-Raphson shooting scheme with RK45 method is utilized to unravel the equations from (7)-(10), under the restriction (11). We convert our BVP to IVP to make it compatible with RK45. The equations (7-11) are converted to first order ordinary differential equations using the following transformations.

$$\varphi_1 = X_1, \quad \varphi_{1_\eta} = X_2, \quad \varphi_{1_{\eta\eta}} = X_3, \quad \varphi_{1_{\eta\eta\eta}} = X'_3, \quad \varphi_2 = X_4, \quad \varphi_{2_\eta} = X_5, \quad \varphi_{2_{\eta\eta}} = X_6,$$
$$\varphi_{2_{\eta\eta\eta}} = X'_6, \quad \varphi_3 = X_7, \quad \varphi_{3_\eta} = X_8, \quad \varphi_{3_{\eta\eta}} = X'_8, \quad \varphi_4 = X_9, \quad \varphi_{4_\eta} = X_{10}, \quad \varphi_{4_{\eta\eta}} = X'_{10}.$$

The obtained system of first order ordinary differential is

$$X'_1 = X_2 \quad (12)$$
$$X'_2 = X_3 \quad (13)$$
$$X'_3 = \frac{\beta\left[\left(\frac{1}{Da}+M\right)(X_2-\lambda_3)+Fr(X_2^2-\lambda_3^2)+(X_2^2-\lambda_3^2)-(X_1+X_4)X_3\right]}{(1+\beta)} \quad (14)$$
$$X'_4 = X_5 \quad (15)$$
$$X'_5 = X_6 \quad (16)$$
$$X'_6 = \frac{\beta\left[\left(\frac{1}{Da}+M\right)(X_5-\lambda_4)+Fr(X_5^2-\lambda_4^2)+(X_5^2-\lambda_4^2)-(X_1+X_4)X_6\right]}{(1+\beta)} \quad (17)$$
$$X'_7 = X_8 \quad (18)$$
$$X'_8 = -Pr[(NbX_{10} + NtX_8)X_8 + (X_1 + X_4)X_8 + Q^*\varphi_3] \quad (19)$$
$$X'_9 = X_{10} \quad (20)$$

$$X'_{10} = -[Sc(X_1 + X_4)X_{10} + NrX'_8] \quad (21)$$

with boundary conditions

$$X_1(0) = X_4(0) = 0, \quad X_2(0) = \lambda_1, \quad X_5(0) = \lambda_2, \quad X_7(0) = 1, \quad X_9(0) = 1$$

$$X_2(\infty) = \lambda_3, \quad X_5(\infty) = \lambda_4, \quad X_7(\infty) = 0, \quad X_9(\infty) = 0. \quad (22)$$

To solve above system of equations, Firstly we pick the limit for $\eta$. Secondly, we chose the initial guesses for $X_3(0)$, $X_6(0)$, $X_8(0)$, and $X_{10}(0) = 0$. Thirdly Runge-Kutta method applied to solve the system. Fourthly it is inspected that if the boundary residual is less than accepted error if not Newton-Raphson method is employed to recalculate the values of $X_3(0)$, $X_6(0)$, $X_8(0)$, and $X_{10}(0) = 0$. The edge of the Runge-Kutta 4th order method over other numerical method is that the implementation of the method is easy. Further, the results are always reliable as the local truncation error for $RK4$ is $O(h^5)$.

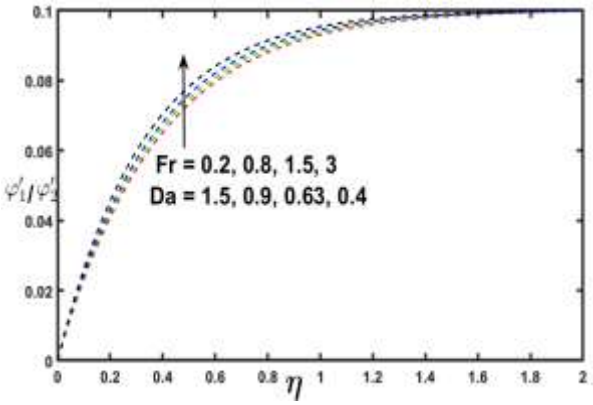


Fig.3: Variability of $\varphi_{1'}$ and $\varphi_{2'}$with $Fr$ and $Da$.

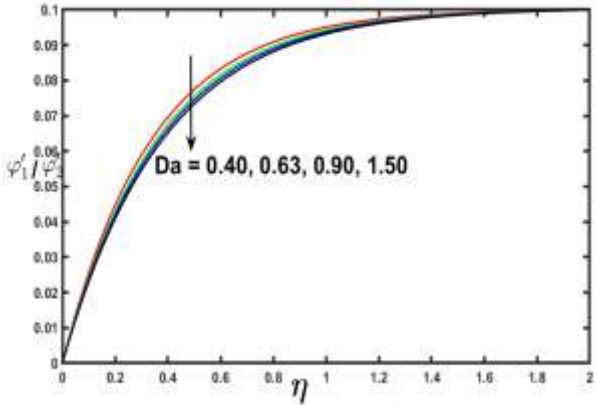


Fig.4:Variability of $\varphi_{1'}$ and $\varphi_{2'}$ with $M$.

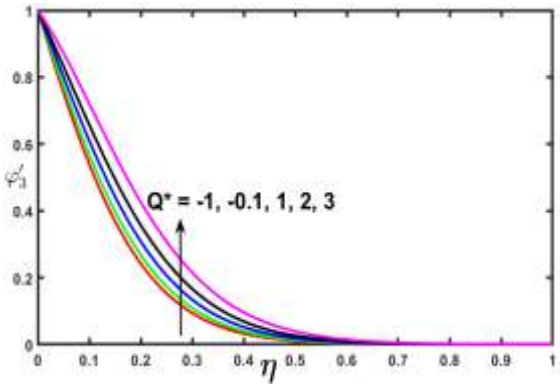


Fig.5:Variability of $\varphi_{3'}$ with heat source ($Q * > 0$) and heat sink ($Q * < 0$)

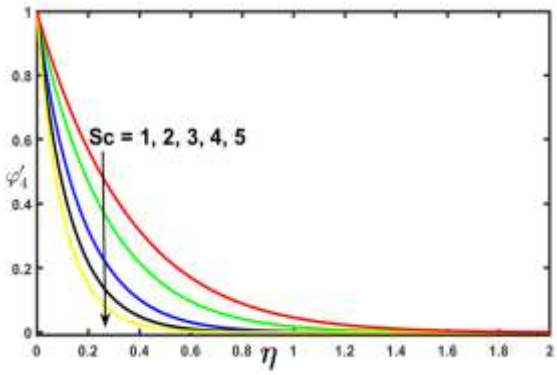


Fig. 6: Variability of $\varphi_{4'}$ with $Sc$.

## 4. Results and discussion

This part of the paper consists of plots which demostrate the impacts of concentration, mass transfer, temperature, heat transfer and velocities under Blasius conditions. Values of $\lambda_1 = \lambda_2 = 0$, $\lambda_3 = \lambda_4 = 0.1$(ifnotmentionedseparately) . If not mentioned separately the values of other parameters in both cases are fixed to $Q^* = 3$, $M = 3$, $Sc = 2$, $Pr = 6.07$, $B = 3$, $Fr = 0.2$, $Da = 0.63$, $Nb = 0.05$ and $Nt = 0.02$.

### 4.1 Variations in velocity

Velocity plots are maintained against the Casson parameter, Darcy number, magnetic

field parameter, and Darcy-Forchheimer number via figures 1-4. It came in to notice that the velocity is increasing with the Casson parameter. Non-Newtonian properties of Casson number enhance the viscosity and curtail the yield stress. This should reduce the velocity of the nanofluid near the surface but contrarily it is increasing because of it has minimal impacts in case of free stream. Boundary layer thickness is noticed shrinking Figure 1. The porous medium permeability is reducing with increasing increments in $Da$ and curtailing with increments in $Fr$. This forces the velocity of the fluid to grow with decreasing $D$a and increasing $Fr$(Please see figure 2-3). Another Figure 4 depicts that the larger electromagnetic force has minimal impacts on free stream velocity. The normally induce magnetic increase in the circular motion of the fluid.

**4.2 Variations in temperature and concentration**

Figure 5 shows the temperature variation with Q*. with reducing heat sink, the temperature is increasing and with increasing heat source temperature is also increasing. It means the heat sources sink can significantly control the temperature. In another figure 6, the Schmidt number forcing the concentration to curtail. Concentration is reducing since the increasing Schmidt number is related to higher dynamic viscosity and low mass diffusivity.

**4.3 Variation in heat and mass transfer**

Figure 7-8 are maintained to depict the nature of heat and mass transfer rate. It is concluded that the heat transfer rate in Casson nanofluid can be enhanced by controlling the heat source and Schmidt number. Also if a heat sink is installed then minimum heat loss will be there(See figure 7). The mass transfer rate can be enhanced by controlling the Schmidt number and Brownian motion.

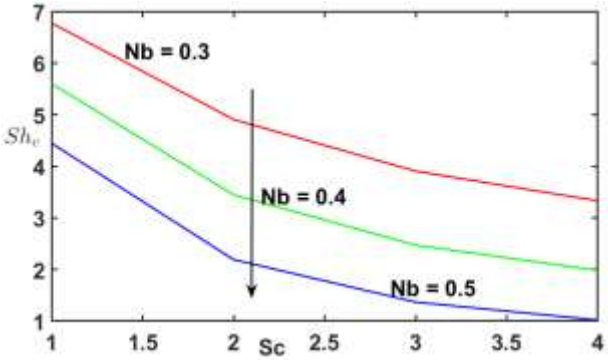


Fig.7: Variability of heat transfer rate with $Q*$ and $Sc$.

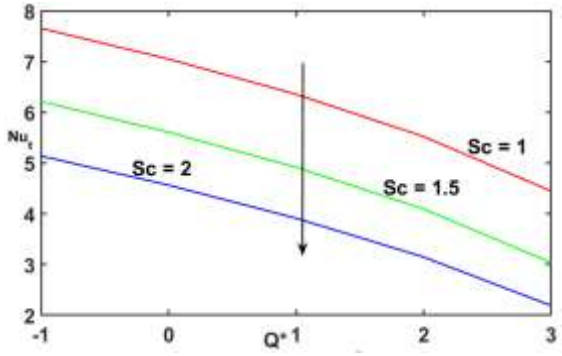


Fig.8:Variability of mass transfer rate with $Nb$ and $Sc$.

## 5. Conclusion

Forchheimer effects on an electrically conducted, 3D Casson nanofluid under Blasisus conditions are studied in this paper. The shooting method(Newton-Raphson) along with RK45 is incorporated. The following observations are important to consider.

• Velocity is depicts the identical behaviour with $M$, $Fr$, and $B$ that is velocity increasing with increment in these parameters but $Da$ has adverse impact.

• Heat transfer rate of Casson nanofluid for Blasisus type flows can be enhanced by controlling heat source and installing a heat sink device.

• Mass transfer rate of Casson nanofluid for Blasisus type flows can be enhanced by controlling the Schmidt number and Brownian parameter.

• Concentration reduction with $Sc$ and temperature enhancement with $Q*$ is noticed.

**References**

[1] P.R.H. Blasius, Grenzschichten in Flüssigkeiten mit kleiner Reibung, Druck von BG Teubner, 1907.

[2] Ludwig Prandtl, Motion of fluids with very little viscosity, (1928).

[3] Adhil Ridha, On the three-dimensional alternative to the Blasius boundary-layer solution, Comptes Rendus Mecanique 333(10) (2005) 768-772.

[4] Y.S. Kachanov, A. Michalke, Three-dimensional instability of the Blasius boundary layer, In Laminar-turbulent transition, Springer, Berlin, Heidelberg (1995) 473-480.

[5] K. Tsigklifis, A.D. Lucey, Global stability of three-dimensional disturbances in blasius boundary-layer flow over a compliant panel, In 19th Australian Fluid Mechanics Conference, Melbourne, Australia (2014).

[6] Chandrasekhar, S., & Woltjer L. (1958). On force-free magnetic fields. National Academy of Sciences, 44 (4) 285-289.

[7] Ledvina, S. A., & Cravens, T. E. (1998). A three-dimensional MHD model of plasma flow around Titan. Planetary and Space Science, 46(9-10), 1175-1191.

[8] Hawley, J. F., Balbus, S. A., & Stone, J. M. (2001). A magnetohydrodynamic nonradiative accretion flow in three dimensions. The Astrophysical Journal Letters, 554(1), L49.

[9] Hayat, T., Qasim, M., & Abbas, Z. (2010). Homotopy solution for the unsteady three-dimensional MHD flow and mass transfer in a porous space. Communications in Nonlinear Science and Numerical Simulation, 15(9), 2375-2387.

[10] Chand, K., & Kumar, R. (2012). Hall effect on heat and mass transfer in the flow of oscillating viscoelastic fluid through porous medium with wall slip conditions. Indian Journal of Pure & Applied Physics, 50, 149-155.

[11] Kumar, R., Sood, S., Raju, C. S. K., & Shehzad, S. A. (2019). Hydromagnetic unsteady slip stagnation flow of nanofluid with suspension of mixed bio-convection. Propulsion and Power Research, 8(4), 362-372.

[12] M. Mustafa, J.A. Khan, T. Hayat, A. Alsaedi, Sakiadis flow of Maxwell fluid considering magnetic field and convective boundary conditions, Aip Advances 5(2) (2015) 027106.

[13] T. Hayat, A. Aziz, T. Muhammad, A. Alsaedi, Darcy–Forchheimer three-dimensional flow of Williamson nanofluid over a convectively heated nonlinear stretching surface, Communications in Theoretical Physics 68(3) (2017) 387.

[14] T. Muhammad, A. Alsaedi, T. Hayat, S.A. Shehzad, A revised model for Darcy-Forchheimer three-dimensional flow of nanofluid subject to convective boundary condition, Results in physics 7 (2017) 2791-2797.

[15] T. Hayat, F. Haider, T. Muhammad, A. Alsaedi, Three-dimensional rotating flow of carbon nanotubes with Darcy-Forchheimer porous medium PloS one 12(7) (2017) e0179576.

[16] Vafai, K. (2010). Porous media: Applications in biological systems and biotechnology. CRC Press, Boca Raton.

[17] Vafai, K., & Tien, C. L. (1981). Boundary and inertia effects on flow and heat transfer in porous media. International Journal of Heat and Mass Transfer, 24(2), 195-203.

[18] Vafai, K., & Tien, C. L. (1982). Boundary and inertia effects on convective mass transfer in porous media. International Journal of Heat and Mass Transfer, 25(8), 1183-1190.

[19] Nield, D. A. (1991). The limitations of the Brinkman-Forchheimer equation in modeling flow in a saturated porous medium and at an interface. International Journal of Heat and Fluid Flow, 12(3), 269-272.